



## Saharan dust aerosol over the central Mediterranean Sea: PM<sub>10</sub> chemical composition and concentration versus optical columnar measurements

M. Marconi<sup>1</sup>, D. M. Sferlazzo<sup>2</sup>, S. Becagli<sup>1</sup>, C. Bommarito<sup>3</sup>, G. Calzolari<sup>4</sup>, M. Chiari<sup>4</sup>, A. di Sarra<sup>5</sup>, C. Ghedini<sup>1</sup>, J. L. Gómez-Amo<sup>5</sup>, F. Lucarelli<sup>4</sup>, D. Meloni<sup>5</sup>, F. Monteleone<sup>3</sup>, S. Nava<sup>4</sup>, G. Pace<sup>5</sup>, S. Piacentino<sup>3</sup>, F. Rugi<sup>1</sup>, M. Severi<sup>1</sup>, R. Traversi<sup>1</sup>, and R. Udisti<sup>1</sup>

<sup>1</sup>Department of Chemistry, University of Florence, Sesto Fiorentino, Florence, 50019, Italy

<sup>2</sup>ENEA, Laboratory for Earth Observations and Analyses, 92010, Lampedusa, Italy

<sup>3</sup>ENEA, Laboratory for Earth Observations and Analyses, 90141, Palermo, Italy

<sup>4</sup>Department of Physics and Astronomy, University of Florence and I.N.F.N., Florence, Via Sansone 1, 50019 Sesto F.no, Florence, Italy

<sup>5</sup>ENEA Laboratory for Earth Observations and Analyses, 00123, Rome, Italy

Correspondence to: S. Becagli (silvia.becagli@unifi.it)

Received: 5 June 2013 – Published in Atmos. Chem. Phys. Discuss.: 14 August 2013

Revised: 14 January 2014 – Accepted: 16 January 2014 – Published: 21 February 2014

**Abstract.** This study aims to determine the mineral contribution to PM<sub>10</sub> in the central Mediterranean Sea, based on 7 yr of daily PM<sub>10</sub> samplings made on the island of Lampedusa (35.5° N, 12.6° E).

The chemical composition of the PM<sub>10</sub> samples was determined by ion chromatography for the main ions, and, on selected samples, by particle-induced X-ray emission (PIXE) for the total content of crustal markers. Aerosol optical depth measurements were carried out in parallel to the PM<sub>10</sub> sampling.

The average PM<sub>10</sub> concentration at Lampedusa over the period June 2004–December 2010 is 31.5 μg m<sup>-3</sup>, with low interannual variability. The annual means are below the EU annual standard for PM<sub>10</sub>, but 9.9 % of the total number of daily data exceeds the daily threshold value established by the European Commission for PM (50 μg m<sup>-3</sup>, European Community, EC/30/1999).

The Saharan dust contribution to PM<sub>10</sub> was derived by calculating the contribution of Al, Si, Fe, Ti, non-sea-salt (nss) Ca, nssNa, and nssK oxides in samples in which PIXE data were available. Cases in which crustal content exceeded the 75th percentile of the crustal oxide content distribution were identified as elevated dust events. Using this threshold, we obtained 175 events. Fifty-five elevated dust events (31.6 %)

displayed PM<sub>10</sub> higher than 50 μg m<sup>-3</sup>, with dust contributing by 33 % on average.

The crustal contribution to PM<sub>10</sub> has an annual average value of 5.42 μg m<sup>-3</sup>, and reaches a value as high as 67.9 μg m<sup>-3</sup> (corresponding to 49 % of PM<sub>10</sub>) during an intense Saharan dust event.

The crustal content estimated from a single tracer, such as Al or Ca, is in good agreement with the one calculated as the sum of the metal oxides. Conversely, larger crustal contents are derived by applying the EU guidelines for demonstration and subtraction of exceedances in PM<sub>10</sub> levels due to high background of natural aerosol. The crustal aerosol amount and contribution to PM<sub>10</sub> showed a very small seasonal dependence; conversely, the dust columnar burden displays an evident annual cycle, with a strong summer maximum (monthly average aerosol optical depth at 500 nm up to 0.28 in June–August). We found that 71.3 % of the dust events identified from optical properties over the atmospheric column display a high dust content at the ground level. Conversely, the remaining 28.7 % of cases present a negligible or small impact on the surface aerosol composition due to the transport processes over the Mediterranean Sea, where dust frequently travels above the marine boundary layer, especially in summer.

Based on backward trajectories, two regions, one in Algeria–Tunisia, and one in Libya, are identified as main source areas for intense dust episodes occurring mainly in autumn and winter. Data on the bulk composition of mineral aerosol arising from these two source areas are scarce; results on characteristic ratios between elements show somewhat higher values of Ca/Al and (Ca + Mg)/Fe ( $2.5 \pm 1.0$ , and  $4.7 \pm 2.0$ , respectively) for Algeria–Tunisia than for Libyan origin (Ca/Al =  $1.9 \pm 0.7$  and (Ca + Mg)/Fe =  $3.3 \pm 1.1$ ).

## 1 Introduction

Mineral aerosol is produced by wind erosion and resuspension in arid and semiarid regions and contributes by about 45 % to the total atmospheric aerosol load (Duce et al., 1991). In particular, the Sahara is the largest source of soil-derived aerosols, with an annual emission estimated to be about  $600 \text{ Tg yr}^{-1}$  (D’Almeida, 1986; Marticorena et al., 1997). By comparison, estimates of global dust emission range from 1000 to  $3000 \text{ Tg yr}^{-1}$  (Zender et al., 2004).

Mineral aerosols affect the atmospheric radiative balance through scattering, absorption, and emission of radiation (IPCC, 2007; di Sarra et al., 2011); they also affect it indirectly, by acting as cloud condensation nuclei (Levin et al., 1996) and modifying cloud properties. The investigation of the role that dust plays on climate is among the main priorities to reduce uncertainties in future climate projections (Engelstaedter et al., 2006).

Dust may also greatly increase the atmospheric levels of PM, adversely affecting air quality. This effect is especially relevant in southern and eastern Europe (Escudero et al., 2005, 2007; Pederzoli et al., 2010; Gerasopoulos et al., 2006, Dayan et al., 1991) due to the transport processes from Africa and the Arabian Peninsula and to the relatively low precipitation, which causes a long residence time of PM in the Mediterranean atmosphere (Querol et al., 2009). Intense dust transport episodes may cause health impacts due to the high levels of PM, with which transport of anthropogenic pollutants may be associated (Erel et al., 2006).

Thus, many recent studies have focused on the estimation of the influence of African dust on air quality in southern European countries, especially Spain and Italy (Rodríguez et al., 2001; Escudero et al., 2007; Perrino et al., 2008, Nava et al., 2012). Recent analyses by Kallos et al. (2007) and Astitha et al. (2008) have shown that, in the period 2001–2005, desert dust is present in approximately 50 % of the days in which the PM<sub>10</sub> EU limit is exceeded.

In addition, dust particles frequently act as reaction surfaces for reactive gases (Dentener et al., 1996; Levin et al., 1996), affecting atmospheric chemical processes. Dust also influences atmospheric chemistry also through modulation of solar radiation, particularly in the ultraviolet spectral range, thus influencing photochemical processes (Casasanta

et al., 2011; Meloni et al., 2003). Furthermore, observations in southern Europe show that the atmospheric deposition of specific nutrients is enhanced by dust input from northern Africa (Avila and Rodà, 2002). Mediterranean marine regions are highly influenced by crustal dust deposition, which may provide large amounts of nutrients for phytoplankton (Béthoux et al., 1996; Guerzoni et al., 1999). However, the processes that control the speciation and cycling of micronutrients in the surface ocean after dust deposition are scarcely known (Baker and Croot, 2010), and the hypotheses about biogeochemical responses to sporadic inputs of dust are controversial (Wagener et al., 2010).

Due to the large number of processes in which dust is involved, the characterization of dust’s evolution and chemical composition is very important, especially in the central Mediterranean Sea, where experimental studies covering long time periods are scarce. In this study we present the evolution of dust markers in aerosol samples collected on the island of Lampedusa throughout the period June 2004–December 2010. The study aims at quantifying the Saharan dust contribution to PM<sub>10</sub> at the ground level and assessing its seasonal evolution, also in comparison with spectral aerosol optical depth, used as an indicator of columnar aerosol burden. Ratios between elements are also used to study the variability of the dust composition, and this variability in relation to main source areas.

## 2 Methods

### 2.1 Sampling

Chemical and physical characterization of the aerosol samples collected at remote sites is crucial to ascertain the influence of natural sources on PM. In this regard, the island of Lampedusa (35.5° N, 12.6° E), which is located in the central Mediterranean Sea at least 100 km from the nearest Tunisian coast, is an ideal sampling site. The island covers a total area of about  $20 \text{ km}^2$ , and is practically devoid of vegetation. About 6000 inhabitants live permanently in Lampedusa, although the number of inhabitants significantly grows during the summer tourist season. Industrial activities (which include a fish canning industry) are very scarce. Local aerosol sources are very low, and the main anthropogenic source arises from ships crossing the Mediterranean Sea about 100 km north of the island (Becagli et al., 2012). The aerosol sampler is positioned on a 45 m a.s.l. plateau on the north-eastern coast of Lampedusa, at the Station for Climate Observations maintained by ENEA (the Italian National Agency for New Technologies, Energy and Sustainable Economic Development). At this site, continuous observations of greenhouse gases (Artuso et al., 2009, 2010), aerosol properties (di Sarra et al., 2011; Meloni et al., 2006; Pace et al., 2006), total ozone (Gómez Amo et al., 2012), ultraviolet irradiance (di Sarra et al., 2002; Meloni et al.,

**Table 1.** Number of PM<sub>10</sub> samples collected in each month from June 2004 to December 2010.

	PM <sub>10</sub> 1 day every three sampling			PM <sub>10</sub> daily resolution			PM <sub>10</sub> 1 day every three sampling
	2004 <i>n</i>	2005 <i>n</i>	2006 <i>n</i>	2007 <i>n</i>	2008 <i>n</i>	2009 <i>n</i>	2010 <i>n</i>
Jan		14*	9*	12	30	27	5
Feb		4*	6*	26	28	16	10
Mar		9*	8*	30	27	29	10
Apr		5*	10*	25	25	25	11
May		9*	13*	31	23	30	11
Jun	4*	9*	10*	30	29	26	8
Jul	15*	9*	10*	26	27	30	13
Aug	8*	9*	9*	30	21	31	11
Sep	8*	9*	1*	27	28	15	11
Oct	8*	9*	5*	17	27	–	9
Nov	8*	9*	8*	8	27	–	13
Dec	15*	10*	8*	30	22	–	2
TOTAL	66	105	97	292	314	229	114
Year Sampling	18	29	27	80	86	63	31
Coverage %							

\* PM<sub>1.0</sub> and PM<sub>2.5</sub> alternating sampling.

2005; Arola et al., 2009; Mateos et al., 2013), surface radiation budget (di Sarra et al., 2008; Di Biagio et al., 2010) and other climatic parameters are carried out. Lampedusa is part of the regional World Meteorological Organization/Global Atmospheric Watch network. Aerosol optical properties are measured with a multi-filter rotating shadow band radiometer (MFRSR; Harrison et al., 1994). The MFRSR is a seven-channel radiometer which measures global and diffuse irradiances, and allows for the determination of column aerosol optical depth at five wavelengths (416, 496, 615, 671, and 869 nm). The measurement details and data retrieval are described by Pace et al. (2006). The aerosol PM<sub>10</sub> daily sampling is carried out by using a low volume sequential sampler (TECORA Skypost) in accordance with EN12341. The sampling campaign was started in June 2004, and alternated in sequence samplings of PM<sub>10</sub>, PM<sub>2.5</sub>, and PM<sub>1.0</sub>. Starting in 2007, only the PM<sub>10</sub> sampling was carried out on a daily basis. The sampling head was periodically cleaned and the stage of impact was covered by thin layer of Molykote grease in order to avoid bouncing of particles larger than 10 μm. Some interruptions occurred during the sampling period due to technical failures. The sample collection was carried out at constant flow of 2.3 m<sup>3</sup> h<sup>-1</sup> over 24 h integration time; 47 mm diameter 2 μm pore Pall Gelman Teflon filters were used. The PM<sub>10</sub> mass concentration was determined with the gravimetric method: filters were weighted before and after sampling, and the sampling volume was provided by the sampler. Before weighing, all filters were conditioned for at least 24 h at a relative humidity of 50 % and a temperature of 20 °C.

Table 1 reports the monthly number of aerosol samples collected during the 2004–2010 period.

## 2.2 Chemical analyses

Each filter was divided into three sections: one largest section (corresponding to half a filter) and two smaller sections (a quarter of filter each). Aerosol from one of the quarters of each filter were extracted using about 10 ml of Milli-Q water in an ultrasonic bath for 15 min, and the ionic load (Na<sup>+</sup>, NH<sub>4</sub><sup>+</sup>, K<sup>+</sup>, Mg<sup>2+</sup>, Ca<sup>2+</sup>, F<sup>-</sup>, Cl<sup>-</sup>, NO<sub>3</sub><sup>-</sup>, SO<sub>4</sub><sup>2-</sup>, methanesulfonate – MS<sup>-</sup>, acetate, formate, glycolate, oxalate) was evaluated by two Dionex DX1000 and one Dionex DX500 ion chromatographs working in parallel (Becagli et al., 2011). The half Teflon filters were analysed by particle-induced X-ray emission (PIXE) technique (Chiari et al., 2005; Lucarelli et al., 2011) in order to obtain the total elemental composition. PIXE measurements were made using the aerosol-dedicated experimental set-up (Calzolari et al., 2006) available at the LABEC laboratory of the National Institute of Nuclear Physics (INFN) in Florence, equipped with a 3 MV Tandemron accelerator. PIXE analysis was carried out on a reduced number of samples; therefore, the total elemental composition is available for a restricted data set (December 2004–December 2005, and January 2007–December 2008).

## 2.3 Backward trajectories

The Hybrid Single-Particle Lagrangian Integrated Trajectory (HYSPPLIT) modelling system (Draxler and Rolph, 2012) was used for the trajectory analysis. The National Centres for Environmental Prediction (NCEP) reanalysis database was

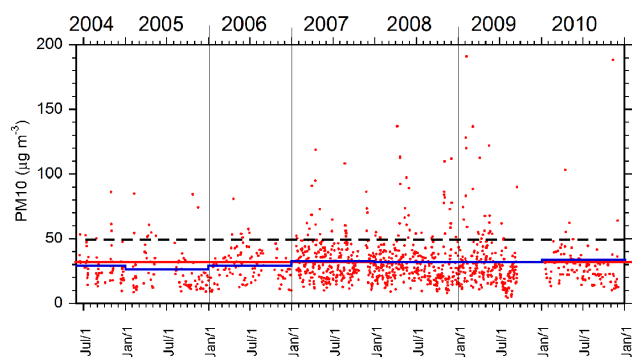


**Fig. 1.** Temporal evolution of  $\text{PM}_{10}$  at Lampedusa in the period June 2004–December 2010. The black dashed line represents the EU daily threshold value of  $50 \mu\text{g m}^{-3}$ . The red line is the mean  $\text{PM}_{10}$  over the whole sampling period and the blue one represent the annual means.

used as meteorological input, with a  $2.5 \times 2.5$  degrees horizontal resolution. Trajectories were used to identify source regions of the collected dust (see Sect. 3.3). The HYSPLIT model was run to compute 72 h back trajectories ending at Lampedusa at 50 m a.g.l. in the middle of the 24 h time interval used for the filter sampling when an elevated amount of crustal material was measured in  $\text{PM}_{10}$ .

### 3 Results and discussion

#### 3.1 $\text{PM}_{10}$ concentration and contribution of crustal aerosol to $\text{PM}_{10}$

##### 3.1.1 $\text{PM}_{10}$ concentration

Figure 1 shows the daily values of  $\text{PM}_{10}$  in the period June 2004–December 2010. The average  $\text{PM}_{10}$  concentration over the considered period is  $31.5 \mu\text{g m}^{-3}$  (average over 1134 samples). In spite of the large day-to-day variability, the mean value agrees with the one measured at Finokalia ( $35.5 \mu\text{g m}^{-3}$ ) and Erdemli ( $36.4 \mu\text{g m}^{-3}$ ), sites of the same typology (natural, rural) in the eastern Mediterranean region (Koçak et al., 2007, and reference therein), but they are much lower than at northern African sites (e.g. Bouchlaghem et al., 2009). Conversely, the overall average is higher than those reported by Pey et al. (2013) for rural background sites across the Mediterranean region for the period 2001–2011. This difference is likely due to the different elevation of the sampled sites and the impact of different sources.

The  $\text{PM}_{10}$  annual mean, even if calculated on different numbers of individual values, shows a relatively limited interannual variability, with values ranging from  $26.1 \mu\text{g m}^{-3}$  in 2005 to  $33.9 \mu\text{g m}^{-3}$  in 2010. Although the  $\text{PM}_{10}$  annual mean is quite high, it is below the EU annual  $\text{PM}_{10}$  standard for  $\text{PM}_{10}$  ( $40 \mu\text{g m}^{-3}$ ); 112 days (corresponding to 9.9 % of the total number of data) exceed the daily thresh-

old value established by the European Commission for  $\text{PM}$  ( $50 \mu\text{g m}^{-3}$ , European Community, EC/30/1999). The percentage of the exceedances is higher than allowed by the EU law ( $35 \text{ days yr}^{-1}$ , corresponding to 9.6 %). It has to be noticed that the EU rules requires that at least 90 % of the days of the year are used to calculate annual mean values and number of exceedances. In our data set however, available data correspond to more than 80 % of the year only for 2007 and 2008.

##### 3.1.2 Dust contribution to $\text{PM}_{10}$

It is known that  $\text{PM}_{10}$  concentrations are strongly influenced by the occurrence of African dust events over the Mediterranean region. In order to quantify the impact of Saharan dust intrusion episodes on  $\text{PM}_{10}$  concentrations, the mineral content was estimated as the sum of the contributions of all the main crustal element oxides ( $\text{SiO}_2$ ,  $\text{Al}_2\text{O}_3$ ,  $\text{Fe}_2\text{O}_3$ ,  $\text{CaO}$ ,  $\text{Na}_2\text{O}$ ,  $\text{MgO}$ ,  $\text{K}_2\text{O}$ ,  $\text{TiO}_2$ ), following the approach reported in the literature by several authors (Eldred et al., 1987; Malm et al., 1994; Miranda et al., 1994; Marcazzan et al., 2001; Nava et al., 2012):

$$[\text{crustalcontent}] = 2.14[\text{Si}] + 1.89[\text{Al}] + 1.43[\text{Fe}]$$

$$+ 1.40[\text{Ca}] + 1.35[\text{Na}] + 1.66[\text{Mg}] + 1.21[\text{K}] + 1.67[\text{Ti}].$$

Some corrections, however, were applied to this formula to take into account the sea-salt contributions to Na, Mg, K, and Ca, which may be relevant at Lampedusa, and possible anthropogenic contributions to the other elements.

In particular, the non-sea-salt (nss)  $\text{Na}^+$ ,  $\text{nssCa}^{2+}$ ,  $\text{nssMg}^{2+}$ , and  $\text{nssK}^+$  fractions were calculated as

$$\text{nssNa} = \text{nssCa} \cdot (\text{Na}/\text{Ca})_{\text{crust}},$$

$$\text{nssCa} = \text{Ca} - \text{ssCa} = \text{Ca} - \text{ssNa} \cdot (\text{Ca}/\text{Na})_{\text{seawater}},$$

$$\text{nssMg} = \text{Mg} - \text{ssMg} = \text{Mg} - \text{ssNa} \cdot (\text{Mg}/\text{Na})_{\text{seawater}},$$

$$\text{nssK} = \text{K} - \text{ssK} = \text{K} - \text{ssNa} \cdot (\text{K}/\text{Na})_{\text{seawater}},$$

where “ss” stands for “sea salt” and

$$\text{ssNa} = \text{Na} - \text{nssNa} = \text{Na} - \text{nssCa} \cdot (\text{Na}/\text{Ca})_{\text{crust}},$$

and where Ca, K, and Mg represent the concentrations of these elements actually measured by PIXE in the samples. Na represents the concentration measured by ion chromatography in each sample. The concentration by ion chromatographic determination was chosen for Na because of the high error in the PIXE measurements for this element. Almost all Na salts are soluble in water, and the soluble fraction can be assumed to coincide with the total concentration. We used the value of 0.56, which is the mean ratio in the Earth’s crust (Bowen, 1979), for  $(\text{Na}/\text{Ca})_{\text{crust}}$  weight to weight [w/w] ratio. The  $(\text{Na}/\text{Ca})_{\text{crust}}$  is expected to vary as a function of the considered dust source region. Different values are reported for lower, bulk, and upper continental crust

(Henderson and Henderson, 2009, Bowen, 1979). In addition, some areas of the Sahara are enriched in Ca minerals (Scheuvs et al., 2013; Desboeufs and Cautenet, 2005; Claquin et al., 1999). The value we used in this work, 0.56, is in the range of those found in the potential source areas affecting Lampedusa aerosol (Scheuvs et al., 2013). However, the impact of using different values of  $(\text{Na}/\text{Ca})_{\text{crust}}$  is limited: the calculated nssCa fraction ranges from 86.7% to 88.1% when  $(\text{Na}/\text{Ca})_{\text{crust}}$  is in the range 0.44–0.95. Values of 0.038, 0.119, and 0.037 were assumed for  $(\text{Ca}/\text{Na})_{\text{seawater}}$ ,  $(\text{Mg}/\text{Na})_{\text{seawater}}$ , and  $(\text{K}/\text{Na})_{\text{seawater}}$ , respectively (Henderson and Henderson, 2009), as they represent the mean ratios in bulk seawater. In the Lampedusa aerosol, the calculated mean non-sea-salt fractions for Na, Ca, Mg, and K are 11.2%, 87.1%, 36.9%, and 65.6%, respectively.

Possible anthropogenic contributions to Al, nssK, and Fe were estimated by calculating the respective ratio to Si, and by deriving the enrichment factors (EFs) with respect to crustal aerosol ratios. The crustal aerosol ratios were calculated with respect to the upper continental crust composition (Henderson and Henderson, 2009). Only few samples present EF higher than 10 for Fe, and about 10% of the samples for nssK. However, since the nssK concentration is very low with respect to the other crustal markers, we used also nssK for the crustal content calculation, instead of recalculating its contribution from other oxides.

Figure 2 shows the temporal evolution of the  $\text{PM}_{10}$  mass concentration and of the crustal oxide content from January 2007 to December 2008, when continuous daily sampling and PIXE analyses were performed, and the percent contribution of dust to the total  $\text{PM}_{10}$ . The average crustal content is  $5.42 \mu\text{g m}^{-3}$ , and reaches values as high as  $67.9 \mu\text{g m}^{-3}$  during intense Saharan dust events. The mean value of crustal aerosol found at Lampedusa is consistent with the decreasing pattern from the eastern to western Mediterranean Basin found by Pey et al. (2013). On the other hand, the mean percentage of crustal aerosol is 17.4%, which is lower than that at other Mediterranean sites (Pey et al., 2012). The relatively low percentage found at Lampedusa is due to the high contribution of other background sources, as explained in Sect. 3.1.3.

Due to the complexity of the instrumentation required for total chemical analysis, and in particular for Si determination, other methods have been proposed for the quantification of Saharan dust content in  $\text{PM}_{10}$ . In particular, Escudero et al. (2007), using only  $\text{PM}_{10}$  measurements, estimated the daily net dust load in  $\text{PM}_{10}$  attributable to an African episode in a given region by subtracting the daily regional background level from the  $\text{PM}_{10}$  concentration. Such a method was accepted by the European Commission to establish guidelines for demonstration and subtraction of exceedances attributable to natural sources under the Directive 2008/50/EC on ambient air quality and cleaner air for Europe ([http://ec.europa.eu/environment/air/quality/legislation/pdf/sec\\_2011\\_0208.pdf](http://ec.europa.eu/environment/air/quality/legislation/pdf/sec_2011_0208.pdf)). The daily regional background

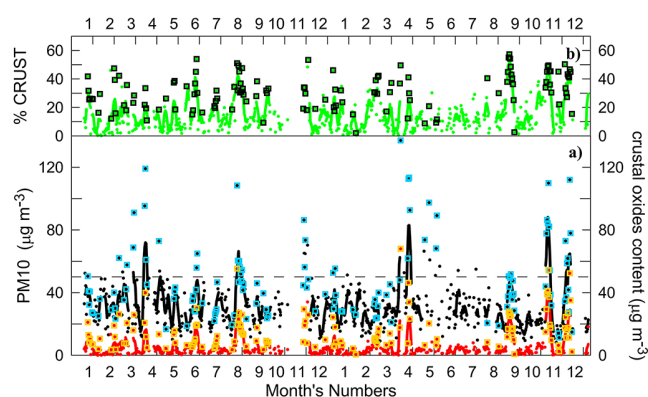


**Fig. 2.** (a) Temporal evolution of the  $\text{PM}_{10}$  mass concentration and of the crustal oxides content for the period January 2007 to December 2008. Daily measurements and 5-day running means are plotted respectively as black (red) dots and lines for  $\text{PM}_{10}$  (crustal content). Measurements having  $\text{nssCa} > 483 \text{ ng m}^{-3}$  are evidenced by cyan and yellow open square for  $\text{PM}_{10}$  and crustal oxides content. (b) Temporal evolution of the mass ratio between crustal oxides content and  $\text{PM}_{10}$  for the period January 2007 to December 2008. Daily measurements and 5-day running means are plotted respectively as green dots and lines, measurements having  $\text{nssCa} > 483 \text{ ng m}^{-3}$  are evidenced by black open squares.

level can be obtained by applying a monthly moving 40th percentile, instead of the less conservative method, using a 30th percentile, by Escudero et al. (2007), to the  $\text{PM}_{10}$  time series at a regional background station after a prior extraction of the data with African dust transport. By using Lampedusa as a regional background station, and by applying this procedure to our data set, we should be able to derive the regional Saharan dust contribution to  $\text{PM}_{10}$ . We compare the regional contribution obtained with this method with the crustal amount derived as the sum of the metal oxides. We obtain a good correlation between the two determinations ( $R = 0.852$ ,  $n = 147$ ). However, the crustal content obtained following the EU guidelines is 1.79 times higher than the one obtained from the sum of the metal oxides. Thus, it appears that the method proposed in the European Community (EC) guidelines for the determination of the Saharan dust contribution to  $\text{PM}_{10}$  is not directly applicable to a site like Lampedusa, which is characterized by a very high contribution of background  $\text{PM}_{10}$ . As will be shown, background  $\text{PM}_{10}$  contributes by about  $26.6 \mu\text{g m}^{-3}$  to the total  $\text{PM}_{10}$  concentration. This value corresponds to the 48th percentile of the whole data set. Thus, the subtraction of the 40th percentile, as proposed by the EC directive, produces an overestimate of the crustal contribution.

Alternatively, the crustal content has been estimated from a single tracer. The most commonly used marker is Al (e.g. Rodríguez et al., 2012, and references therein), which is assumed to represent 8.2% of the upper continental crust (Henderson and Henderson, 2009). We obtain a very good

**Table 2.** Mean concentration and standard deviation of the main component of PM<sub>10</sub> for dust and non-dust cases selected by nssCa concentration (see text). Numbers in brackets are the percentage of the component in the PM<sub>10</sub>.

	Dust cases (167 samples)	Non-dust cases (521 samples)
PM <sub>10</sub>	45.6 ± 24.1 μg m <sup>-3</sup>	26.6 ± 10.8 μg m <sup>-3</sup>
Crustal aerosol	14.6 ± 11.3 μg m <sup>-3</sup> (32.1 %)	2.5 ± 2.4 μg m <sup>-3</sup> (9.6 %)
Sea-salt aerosol	8.1 ± 6.7 μg m <sup>-3</sup> (17.8 %)	8.8 ± 6.9 μg m <sup>-3</sup> (33.2 %)
nssSO <sub>4</sub> <sup>2-</sup>	3.7 ± 2.3 μg m <sup>-3</sup> (7.7 %)	2.6 ± 1.9 μg m <sup>-3</sup> (9.8 %)
NH <sub>4</sub> <sup>+</sup>	0.62 ± 0.51 μg m <sup>-3</sup> (1.4 %)	0.67 ± 0.42 μg m <sup>-3</sup> (2.5 %)
NO <sub>3</sub> <sup>-</sup>	2.6 ± 1.5 μg m <sup>-3</sup> (5.6 %)	1.9 ± 1.0 μg m <sup>-3</sup> (7.3 %)
Unknown	15.9 ± 11.6 μg m <sup>-3</sup> (35.0 %)	10.0 ± 5.2 μg m <sup>-3</sup> (37.6 %)

agreement between the Al-derived and the metal-oxide determinations of the crustal content:  $R = 0.984$ ,  $n = 698$ , slope = 1.0.

Another tracer used to estimate the crustal content is total or nssCa (Putaud et al., 2004; Sciare et al., 2005; Guinot et al., 2007; Favez et al., 2008). Non-sea-salt Ca is not a univocal tracer for dust; in addition, there is a large variability in the crust Ca content. However, nssCa is largely used because it allows the identification and quantification of Saharan dust on the basis of ion chromatographic measurements. Previous studies derived and used calcium-to-dust conversion factors to estimate the crustal content. Sciare et al. (2005) found a value of  $11.0 \pm 1.0\%$  for this factor during the Mediterranean Intensive Oxidant Study (MINOS) campaign in Crete. Favez et al. (2008) derived factors of  $7.6 \pm 9\%$  and  $8.7 \pm 23\%$  at Cairo city by applying the method proposed by Guinot et al. (2005) and using total Ca instead of nssCa.

Although the nssCa determined by ion chromatography in the PM<sub>10</sub> sampled at Lampedusa is about 75 % of the total Ca during Saharan dust events, it displays a good correlation with the crustal content computed by the main crustal element oxides formula ( $R = 0.845$ ,  $n = 688$ ,  $p < 0.01$ ). The slope of the regression line provides the calcium-to-dust conversion factor; here we found a slope of  $10.0 \pm 2\%$ , which is in agreement with previous determinations in the Mediterranean.

### 3.1.3 Elevated dust cases

A criterion based on the crustal content was defined with the aim of identifying elevated Saharan dust events. Cases with

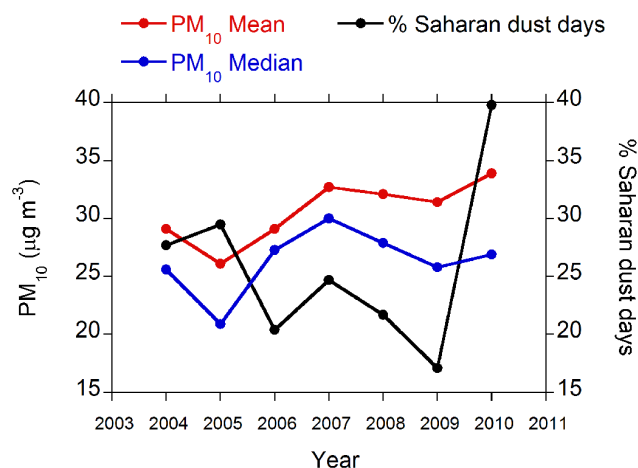


**Fig. 3.** Annual PM<sub>10</sub> mean (red dots) and median (blue dots) on the left y axis. Percentage of Saharan dust episodes (black dots and right y axis) revealed by nssCa for the period 2004–2010.

crustal content exceeding the 75th percentile of the crustal oxide content distribution (corresponding to  $5.44 \mu\text{g m}^{-3}$ ) were identified as elevated dust events. Using this threshold we identify 174 samples characterized by a strong crustal contribution; on the average, dust constitutes 34 % of the PM<sub>10</sub> during these events. However, PIXE analyses are available over a limited time interval, and we defined a criterion based on the amount of nssCa measured with ion chromatography. We classify all cases with nssCa exceeding the 75th percentile of the nssCa distribution as elevated dust events; in this threshold, nssCa<sub>th</sub> corresponds to  $483 \text{ ng m}^{-3}$ . The selection based on this threshold is slightly more restrictive than the one based on the total crustal content. Indeed, by using the two criteria when both measurements are performed, we found that the samples exceeding nssCa<sub>th</sub> are 85 % of those exceeding the 75th percentile of the total crustal content. Back-trajectory analyses show that all the events with nssCa > nssCa<sub>th</sub> are characterized by air masses originating from the Sahara, indicating that the high level of nssCa is not due to local dust resuspension.

Using nssCa measurements, we identify 273 Saharan dust episodes over the period 2004–2010. Figure 3 displays the annual evolution of the mean and median PM<sub>10</sub>, and of the annual frequency of occurrence of elevated dust cases. There is a large interannual variability in the frequency of occurrence of elevated dust events. This variability partly also affects the PM<sub>10</sub> annual behaviour, indicating that the dust plays a central, although not exclusive, role in determining PM<sub>10</sub>. The highest values of PM<sub>10</sub> in 2007 and 2010 correspond with the highest frequencies of Saharan dust days. In particular, 2010 is characterized by a high number of low-intensity Saharan dust intrusions. One exception is constituted by 2005, when a high percentage of Saharan dust days corresponds with a low value of PM<sub>10</sub> mean and median.

This is mainly due to several very low values of  $PM_{10}$  that are able to reduce the annual mean.

Table 2 reports mean values of the main components of PM for elevated dust and remaining cases, as identified on the basis of nssCa. As expected, the concentration of crustal aerosol is about 6 times higher in the dust cases than in non-dust cases. By comparison, the crustal aerosol measured at Crete in the period 2004–2006 accounts for  $80 \mu\text{g m}^{-3}$  (corresponding to 72 % of  $PM_{10}$ ) and  $6 \mu\text{g m}^{-3}$  (37 % of  $PM_{10}$ ) in the dust and non-dust period respectively (Kaloury et al., 2008).

Sea-salt aerosol is the second-most abundant component in elevated dust cases and the first in the remaining cases. The mean amount of sea-salt aerosol, as expected, does not significantly vary between elevated dust and non-dust cases. We have to notice the high amount of unknown mass, higher in dust than in non-dust cases. This is mainly due to a possible large contribution of organic compounds, not determined in these samples. In addition, a certain amount of water bound to hygroscopic aerosol particles and to crustal material, that is not lost during drying procedure before the weighting of the filter, could give a significant contribution to  $PM_{10}$  (Tsyro, 2005; Canepari et al., 2013). The mean amount of the anthropogenic compounds  $\text{NO}_3^-$  and  $\text{nssSO}_4^{2-}$  and, possibly, organic compounds (included in the unknown mass) is larger in dust than in non-dust cases. This behaviour supports the suggestion by Rodriguez et al. (2011) about the possible transport of anthropogenic PM components from polluted areas in northern Africa during dust cases.

The average non-crustal  $PM_{10}$  concentration, obtained by subtracting the crustal content from the total  $PM_{10}$  concentration, is  $25.7 \mu\text{g m}^{-3}$  (average over 698 samples measured during the years when PIXE data are available). Out of this data set, 68  $PM_{10}$  values are higher than  $50 \mu\text{g m}^{-3}$  (9.7 % of the total, a similar percentage to the one found for the whole 2004–2010 data set), while 29 values (4.2 % of the total) of non-crustal  $PM_{10}$  exceeded the threshold. In order to understand the causes for such exceedances, it has to be considered that sea spray accounts for  $8.1 \mu\text{g m}^{-3}$  (17.8 % of  $PM_{10}$ ) as average during dust events (Table 2), and for  $18.7 \mu\text{g m}^{-3}$  on days when the non-crustal  $PM_{10}$  is higher than  $50 \mu\text{g m}^{-3}$ .

### 3.1.4 Surface versus column dust load

A different dust identification methods was adopted in past studies based on ground-based measurements of column aerosol optical properties (Meloni et al., 2007) and air mass back-trajectory analysis (Pace et al., 2006; Pederzoli et al., 2010). This method is applied to the same period when surface PM data are available, and the results are compared with those obtained from the  $PM_{10}$  chemical analyses.

A characterization of the aerosol types present over the atmospheric column can be based on measurements of the aerosol optical depth at 495.7 nm ( $\tau$ ) and the Ångström exponent ( $\alpha$ ) calculated from the aerosol optical depth at 415.6 nm

and 868.7 nm. While  $\tau$  is directly proportional to the aerosol column density (number of particles),  $\alpha$  mainly depends on the particle size distribution (low values of  $\alpha$  indicate a prevailing impact of coarse particles). The combined use of  $\tau$  and  $\alpha$  allows for the identification of different aerosol types, including dust; usually, high values of  $\tau$  associated with low values of  $\alpha$  are typical of Saharan dust (Pace et al., 2006).

Figure 4 shows the behaviour of daily average values of  $\alpha$  versus  $\tau$  for cloud-free conditions for those days in which ionic composition measurements are available in the time period between June 2004 and December 2010. The average values are calculated for the duration of each daily sampling. The reader is reminded that measurements of  $\tau$  are available only during daytime and in cloud-free conditions (see e.g. Meloni et al., 2007). A total of 776 pairs of daily column and surface measurements are obtained. Red markers identify the 193 (i.e. 24.9 % of the total) days with elevated dust amount selected on the basis of the nssCa content. As suggested by Pace et al. (2006), the combined thresholds of  $\tau > 0.15$  and  $\alpha < 0.5$  are used to identify Saharan dust events from the column optical properties. We found that 71.3 % (129 episodes) of the events identified using the optical properties (181, i.e. 23.3 % of the total) display a high nssCa concentration, while 28.7 % of the dust events selected by  $\alpha$  and  $\tau$  present low concentrations of nssCa. A plausible reason for these results is that Saharan dust transport may occur above the marine boundary layer, with small impact on the surface aerosol properties. This situation typically occurs in summer due to the strong vertical convective flows over dust source region (Gobbi et al., 2000; Papayannis et al., 2008; Di Iorio et al., 2009).

Considering the dust events selected on the basis of nssCa, 55.4 % (i.e. 107 episodes) of the cases present  $\alpha$  and  $\tau$  outside of the expected range for dust events. In these cases the Saharan dust intrusion occurs only in the lower atmospheric layers, and the column optical properties are determined by the other aerosol types present in the lower and mid troposphere. The presence of polluted air masses or biomass-burning particles, characterized by high values of the Ångström exponent (Pace et al., 2005; di Sarra et al., 2008), mixed with desert dust or present at different altitudes, may in particular explain the cases with elevated nssCa and  $\alpha > 0.5$ .

We used more restrictive threshold values for  $\tau$  and  $\alpha$  ( $\tau > 0.25$  and  $\alpha < 0.35$ ) in order to identify cases in which Saharan dust is largely dominant over the column. The number of events complying with this limits decreases dramatically, from 181 to 80 (i.e. 10.3 % of the total). About 62.5 % of these 80 events display  $\text{nssCa} > 483 \text{ ng m}^{-3}$ . However, no significant correlation between  $\tau$  and  $PM_{10}$  or nssCa is found, suggesting that, even when the dust is very likely present in the lower and mid-troposphere simultaneously, the behaviour observed at the surface is generally decoupled from what takes place above.

**Table 3.** Seasonal occurrence of different transport scenarios identified on the basis of nssCa on PM<sub>10</sub> and  $\tau$  and  $\alpha$  from optical measurements. The number of cases and the percent with respect to the total number of PM<sub>10</sub> measurements are reported for each season. Four criteria (1 through 4) to detect dust presence in the column and at surface are established, while their combination is used to identify six possible scenarios (a through f) of dust transport. Surface and large surface desert dust episodes correspond to values of nssCa larger than 483 and 2\*483 ng m<sup>-3</sup>, respectively. Episodes characterized by the dominant presence of desert dust aerosol on the atmospheric column are identified when  $\tau > 0.15$  and  $\alpha < 0.5$ , while intense transport episodes are defined when  $\tau > 0.25$  and  $\alpha < 0.35$ . Please note that the percentages in 1–4 refer to the number of occurrences in each season, while those in a–f refer to the number of cases in 1–4.

Periods	DJF	MAM	JJA	SON
Number and frequency of cases	133 (17.1 %)	229 (29.5 %)	271 (34.9 %)	143 (18.4 %)
1) Surface episode	37 (27.8 %)	68 (29.7 %)	46 (17 %)	42 (29.4 %)
a) Columnar episode	7 (18.9 %)	39 (57.4 %)	21 (45.6 %)	19 (45.2 %)
2) Large surface episode	23 (17.3 %)	36 (16 %)	13 (4.8 %)	24 (16.9 %)
b) Columnar episode	7 (30.4 %)	24 (66.6 %)	9 (69.2 %)	15 (62.5 %)
c) Large column episode	1 (4.3 %)	13 (36.1 %)	9 (69.2 %)	7 (29.2 %)
3) Columnar episode	8 (6 %)	66 (28.8 %)	77 (28.4 %)	30 (21 %)
d) Surface episode	8 (100 %)	49 (74.2 %)	43 (55.9 %)	29 (96 %)
4) Large columnar episode	1 (0.75 %)	33 (14.4 %)	36 (13.3 %)	10 (7 %)
e) Surface episode	1 (100 %)	23 (69.7 %)	18 (50.0 %)	8 (80 %)
f) Large surface episode	1 (100 %)	13 (39.4 %)	9 (25 %)	7 (70 %)

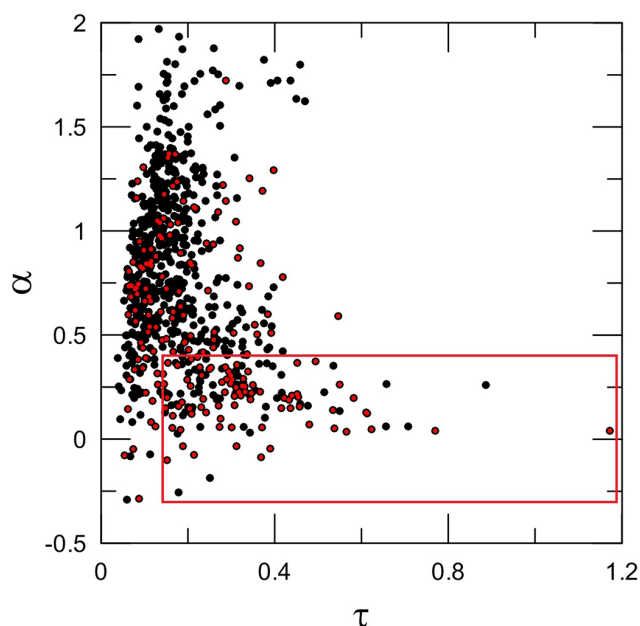


**Fig. 4.** Averages of the aerosol Ångström exponent versus aerosol optical depth at 495.7 nm during the period June 2004–September 2010 for the days with PM<sub>10</sub> ion analyses and for cloud-free periods, when aerosol optical depths measurements are possible. The red dots represent days with nssCa > 483 ng m<sup>-3</sup>, i.e. elevated dust at the surface. The dots inside the red square represent the Saharan dust events selected by  $\tau > 0.15$  and  $\alpha < 0.5$  as reported in Pace et al., (2006).

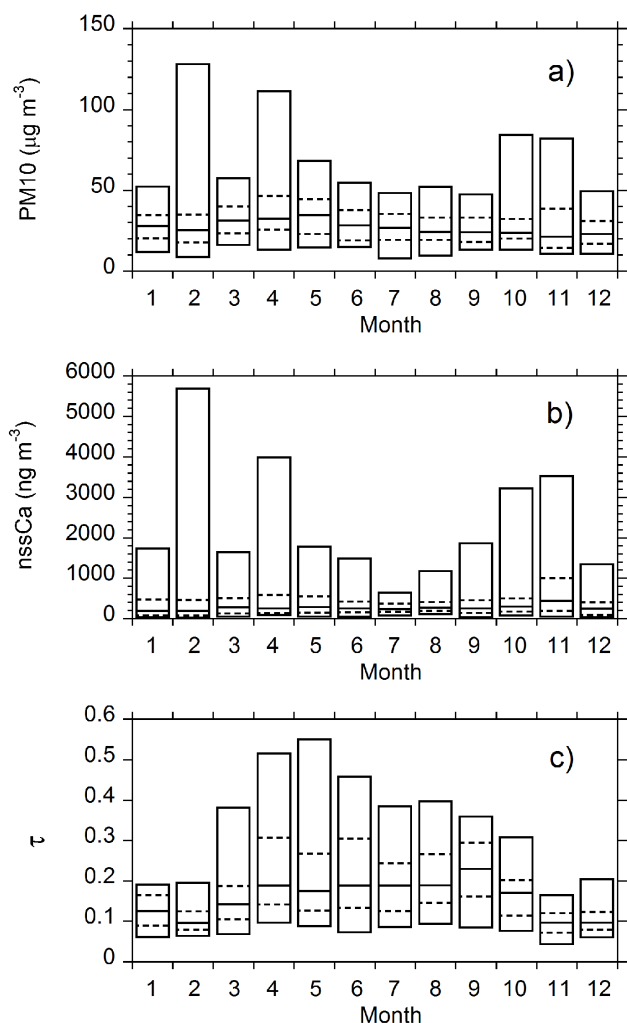
### 3.2 Seasonality of PM<sub>10</sub> and Saharan dust events

Figure 5 shows the monthly distribution of PM<sub>10</sub>, nssCa, and  $\tau$  for the period June 2004–December 2010.

The median values of PM<sub>10</sub> and nssCa show no evident seasonal pattern. The monthly variability is lower during summertime. PM<sub>10</sub> appears marginally higher during spring. Nevertheless, peaks in the 95th percentile occur in the same months for both PM<sub>10</sub> and nssCa, confirming that very high PM<sub>10</sub> values are associated with dust when the marine boundary layer shows a weaker separation from the free troposphere.

Figure 6 reports the percentage of days of elevated Saharan dust occurring in each month as estimated from the column optical properties and from nssCa, and the number of days with PM<sub>10</sub> > 50 µg m<sup>-3</sup>. The percentage of PM<sub>10</sub> exceedances shows two maxima, in May and November; only the latter corresponds to a high occurrence of Saharan dust events as revealed by nssCa. Other sources have to be considered to explain the high percentage of exceedances in May. The Saharan dust days at the ground level show a high occurrence of events in March–April and October–November, and a minimum of the occurrences in summer. Besides, the intensity of Saharan dust surface events in February, April, and October–November is higher than in the other months, as observed by the high values of the 95th percentile in Fig. 5. The minimum in the percentage of Saharan dust events in summer was not observed at other sites in the central Mediterranean (Pey et al., 2013).

The aerosol optical depth shows a totally different seasonal pattern with respect to PM<sub>10</sub> and nssCa. It is characterized by a marked seasonal cycle with maxima in spring–summer. Previous studies reported that the dust optical depth and vertical distribution show a large seasonal cycle, with elevated  $\tau$  and a wider vertical extension in spring and summer; the seasonal change is mainly controlled by dust transport occurring over the boundary layer (Di Iorio et al., 2009).



**Fig. 5.** Monthly distribution of  $\text{PM}_{10}$  (a),  $\text{nssCa}$  (b), and  $\tau$  (c) for the period June 2004–December 2010. The top and bottom of each box show the 5th and 95th percentiles. The middle line shows the median value, and the dashed lines show the 25th and 75th percentiles.

The main dust transport mechanisms prevailing in the western, central, and eastern parts of the Mediterranean Basin and the distribution of the most active source regions produce marked differences in the seasonal evolution of the aerosol optical depth (e.g. Israelevich et al., 2002). The annual maximum in the aerosol optical depth occurred in summer in the western basin, and in early spring in the eastern basin. Two maxima, in spring and in summer, are observed in the central Mediterranean, as also confirmed by the measurements at Lampedusa.

Since  $\tau$  provides information on the entire air column, as discussed above, high values of  $\tau$  in spring and summer do not necessarily imply that a high aerosol load is present close to the surface, where  $\text{PM}_{10}$  and  $\text{nssCa}$  are measured.

Indeed, Fig. 6 shows a very different annual pattern of the percentage of Saharan dust days identified from chemical

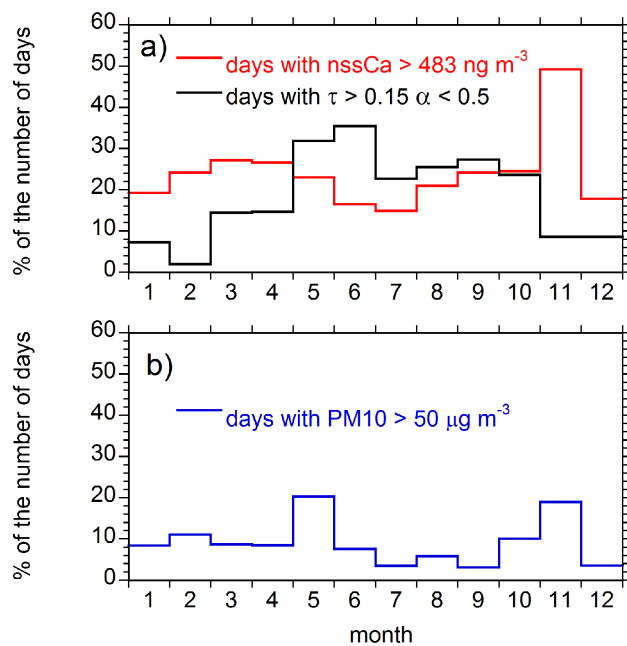


**Fig. 6.** a) Percentage of Saharan dust events observed in each month identified from the aerosol optical properties (black line) and from the  $\text{nssCa}$  amount (red line) and (b) percent number of days with  $\text{PM}_{10} > 50 \mu\text{g m}^{-3}$ .

and optical properties. The seasonal pattern of Saharan dust events identified by optical properties shows a well-defined summer maximum, and in this season the difference between the results of the two methods (optical and chemical) is largest. This evidence suggests, as previously discussed, that in summer air masses coming from Saharan desert overpass the boundary layer over Lampedusa, and no significant mixing between inside and above the boundary layer occurs. A previous study showed that African dust episodes in the western and central parts of the Mediterranean Basin have lower intensity in summer than in the other seasons; they also occur at high altitude, in part due to the presence of the Atlas Mountainous barrier (2500 km extension and peak altitudes up to more than 4000 m a.s.l.), which plays a dominant role in local and mesoscale atmospheric circulation (Pey et al., 2013).

The occurrence of elevated dust at the surface and as columnar values is estimated separately for each season in order to identify a seasonal dependence in the transport processes. Table 3 reports the seasonal occurrence of different dust transport patterns occurring at Lampedusa. Elevated ( $\text{nssCa} > \text{nssCa}_{th}$ ) and large ( $\text{nssCa} > 2$  times  $\text{nssCa}_{th}$ ) surface events are identified based on  $\text{nssCa}$  values, while columnar dust and intense dust episodes are defined on the basis of measurements of the aerosol optical depth and Ångström exponent.

During the winter season, surface and columnar episodes appear decoupled, even when only large surface or columnar

episodes are considered. On the other hand, the few intense columnar episodes always correspond with elevated dust at the surface, suggesting that the aerosol flows at low altitudes and that a strong separation between marine boundary layer and free atmosphere does not exist. The reader should note that during this season, cloudiness represents an important limiting factor for the detection of desert dust from optical measurements.

Spring and autumn present a similar behaviour. Surface episodes occur in 29 % of observations and appear to be independent of columnar episodes, which are detected respectively in 57 % and 45 % of the cases; larger correspondences appear when intense columnar episodes are considered (66.6 % and 62.5 % respectively), although a large number of cases are still observed only at the surface.

As in winter, in the spring and autumn seasons columnar episodes often correspond with presence of dust at the surface, particularly in autumn (96 % of correspondence).

In summer, surface episodes present almost the same frequency of occurrence if we consider the class of dust cases with (45.6 %) or without (54.4 %) simultaneous columnar episodes. Large surface events occur during a columnar episode in 70 % of the cases.

This suggests that when large amounts of dust are present on the column, the penetration in the marine boundary layer may be favoured, especially for long-lasting episodes.

Unlike in the other seasons, in summer columnar events do not necessarily correspond to surface events, and the correspondence further decreases when intense columnar episodes are taken into account.

In summer the presence of dust at surface and on the whole column shows the minimum correspondence, supporting the idea that the strength of the summer convection over the Sahara injects desert dust at high altitudes and those particles, advected over the stable marine boundary layer, seldom influence the surface aerosol amount. The vertical structure of the planetary boundary layer at Lampedusa shows a strong seasonal variability. As shown by Pace et al. (2012), the summer atmosphere is characterized by relatively strong inversions, which reduce the permeability of the lowest atmospheric layers to the penetration of dust.

Several studies have been dedicated to study the meteorological conditions leading to dust transport towards the Mediterranean (e.g. Israelevich et al., 2002; Engelstaedter et al., 2006; Meloni et al., 2008). Most of these studies, however, are based on satellite or column aerosol measurements, and do not differentiate between low altitude and free-tropospheric transport of dust. Engelstaedter et al. (2007) have emphasized that dust mobilization in the Sahara is linked to small scale high winds events. Transport towards the Mediterranean is partly modulated by the inter-tropical convergence zone seasonal changes, leading to the activation of northern African dust source regions during spring and summer. As discussed by Meloni et al. (2008), intense dust events in the central Mediterranean are produced by

the contrast of synoptic systems. In spring and summer, intense transport is mainly governed by a trough extending near the Atlantic coast of Europe and a high-pressure system over northern Africa, generally above 25° N. In winter strong dust transport occurs in association with low pressure systems centered over Portugal, central/northern Europe, and the western Mediterranean.

As also shown by the previous analysis on the seasonal behaviour of the dust events at the surface and in the whole column, the summer inversions over the sea, coupled with strong convection occurring over the desert, produce a decoupling of the surface and free tropospheric cases. Conversely, this decoupling is much smaller in winter and the intermediate seasons (spring and autumn).

### 3.3 Source areas of Saharan dust aerosol

As discussed in Sect. 2.3, the HYSPLIT model was run to compute 72 h back trajectories ending at Lampedusa at 50 m a.g.l. at the centre of the time interval of the filter samples. Trajectories were calculated for the days in which the measured nssCa exceeded 483 ng m<sup>-3</sup>. Given the distribution of the calculated trajectories, two sectors were selected as the main source regions for surface dust episodes. The two sectors are shown in Fig. 7, and correspond to the Algeria–Tunisia region, and to the Libyan area. Each sector includes an important distinct dust source area, as identified by previous studies (Israelevich et al., 2002; Scheuvens et al., 2013). A sector was classified as main source region for each trajectory, and thus for the dust collected at Lampedusa on the arrival day of the trajectory, if the air mass spent more than 50 % of the trajectory time over that sector (50 % permanence criterion).

Given the difficulty in associating a specific source area with a trajectory, especially if the air mass is consistently travelling within the boundary layer (as it is often the case), and given the distribution of the trajectory patterns, no information can be derived for other important source areas from this data set.

Of the total number of samples on which PIXE analysis was carried out, and with nssCa > 483 ng m<sup>-3</sup>, 34 % were associated with a source region in northern Africa: in particular, 21 % of the trajectories were classified as originating from Algeria–Tunisia, and 13 % as coming from Libya. Trajectories that spend most of their time over other areas, such as the Mediterranean Sea or Europe, were also found. These were disregarded in this analysis because, as discussed above, it was not possible to identify a specific source region.

Trajectories originating from the two source regions are mainly found in autumn and winter (76 % of the cases). The Algeria–Tunisia region is the predominant source (26 %) with respect to Libya (9 %) in winter, while the contribution from both regions is comparable (24 % for Algeria–Tunisia and 19 % for Libya) in autumn.

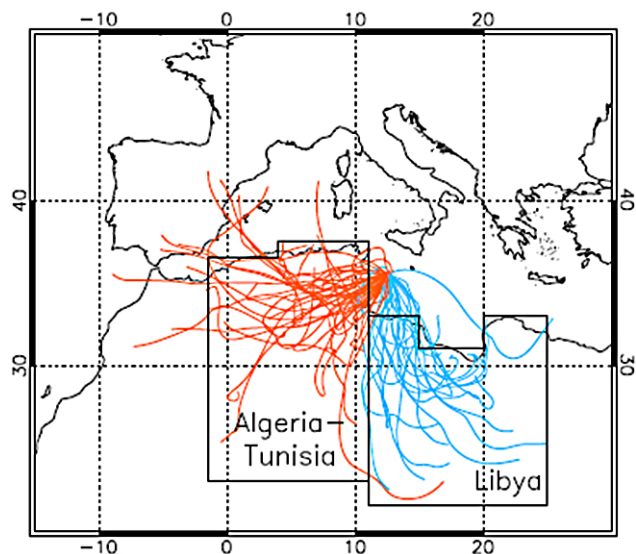


**Fig. 7.** Dust source regions and back trajectories fulfilling the 50% permanence criterion for each source region (orange for Algeria–Tunisia and blue for Libya).

Different ratios between the elements could be considered to identify regional differences in the dust elemental composition; here we prefer to normalize the element abundances to Al in order to compare our data with recent literature data (Scheuvens et al., 2013).

Si and Al are the dominant elements (e.g. Scheuvens et al., 2013) in northern African dust and sediments. The median Si/Al ratio of the Saharan dust events detected from our measurements is  $2.33 \pm 0.17$ , and presents a low variability. Such a ratio is characteristic of a mixture of quartz and aluminosilicates (feldspar, clay minerals), typical of the Sahara.

The average northern African dust composition exhibits Si, Fe, and Mg relative contents comparable to those of the upper continental crust. Northern Saharan dust is slightly depleted in the alkali metals K and Na, and enriched in Ti and P with respect to the upper continental crust, but the ratios between these element and Al do not show significant variations over the Saharan region. Thus, the most useful ratios to discriminate the dust source areas are Ca/Al, Mg/Al, Fe/Al, and especially the elemental ratio (Ca+Mg)/Fe, which shows a pronounced north–south gradient with highest ratios in north-western Africa (Scheuvens et al., 2013).

Figure 8 reports the percentile distributions of the above-mentioned ratios for the Saharan dust episodes divided for the two source areas derived from the trajectory analysis. The Ca/Al, Mg/Al and (Ca+Mg)/Fe ratios are calculated using the non-sea-salt fractions of Ca and Mg, because the uptake of sea salt during transport could produce an increase in the total concentration of these elements, which would not be due to the different Saharan source areas.

Figure 8 shows that both source areas display Ca/Al and Mg/Al ratios higher than the mean crustal composition. The

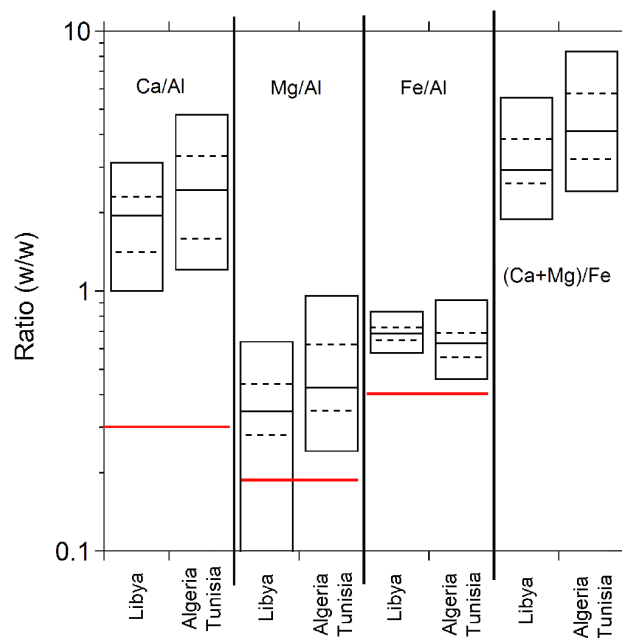


**Fig. 8.** Percentile distribution of Ca/Al, Mg/Al, Fe/Al and (Ca+Mg)/Fe ratios for the two dust source regions evidenced in Fig. 7. The top and bottom of each box show the 5th and 95th percentiles. The middle line shows the median value, and the dashed lines show the 25th and 75th percentiles.

high Ca/Al are related to the elevated carbonate contents in the Saharan sediments, found in north-western (Morocco and Atlas region; Criado and Dorta, 2003; Khiri et al., 2004; Linke et al., 2006; Moreno et al., 2006; Castillo et al., 2008) and north-eastern Africa (Egypt, Libya; Linke et al., 2006, Israel, Ganor and Foner, 1996, Jordan, Abed et al., 2009). Intermediate values were reported for southern Egypt and northern Sudan (Tomadin et al., 1989; Sharif, 1995), while lower Ca contents ( $\text{Ca}/\text{Al} < 0.5$ ) were found in samples from central and southern Algeria and the Sahel zone. The amount of calcite within the silt fraction (Desboeufs and Cautenet, 2005) increases from  $< 5\%$  in the sub-Saharan region to more than  $10\%$  in the northernmost part of northern Africa, with maxima in northern Libya ( $> 15\%$ ). The other Ca mineral (Gypsum) generally exhibits a lower abundance ( $< 2\%$ ) with respect to carbonate, with some local exceptions (northern Libya, central Algeria; Scheuvens et al., 2013).

The Mg content in dust and soil generally correlates with the Ca content. Thus, higher Mg/Al ratios and higher Mg enrichment factors were also reported for the Atlas region ( $\text{Mg}/\text{Al} > 0.3$ ) and for the eastern Mediterranean ( $\text{Mg}/\text{Al} > 0.3$ ). The correlation of Ca and Mg most likely results from the association of the carbonates calcite and dolomite in source sediments, but may also be due to the preferential occurrence of additional palygorskite (a Mg-bearing clay mineral) in areas with higher carbonate contents.

Thus, the northern regions of the Sahara are expected to be enriched in Ca and Mg, although data of bulk composition from Tunisia are missing (Scheuvens et al., 2013). Figure 8 shows that, in spite of the very large variability, the Tunisia–Algeria dust source area presents Ca/Al and Mg/Al ratios somewhat higher than the Libyan source. (Ca+Mg)/Al or (Ca+Mg)/Fe are also relevant ratios to discriminate between different source areas. As shown by Scheuvens et al. (2013), the mean value of (Ca+Mg)/Fe is higher (equal to 4.8) for Algeria–Tunisia than for southern Algeria (values of 0.6–1.2), and for the regions of Mali and Mauritania (Escudero et al., 2011). The areas in the sub-Saharan region present a still lower (Ca+Mg)/Fe ratio (<0.85). Therefore, due to the Fe content differences between north-western and north-eastern Saharan source regions, the ratio (Ca+Mg)/Fe may help to assign northern African dusts to a specific source region. Indeed, quite different median values for Algeria–Tunisia (4.1) and Libya (2.9) source areas are found in our data set, as shown in Fig. 8.

It must be pointed out, however, that the retrieved results are characterized by a very large variability, and the distributions of the ratios we used overlap in most cases. This very high variability may depend on the uncertainties implied in the attribution of the air mass trajectories to the source areas. Here we applied the permanence criterion to increase the probability that the sampled dust was produced in the identified region. However, uncertainties in the trajectories are expected to be large, due to the low resolution of the meteorological data, the lack of meteorological measurements over the Sahara, and the possible role of temporal variations in the trajectories during the sampling time, which are not taken into account. In addition, long-range transport of dust over the Sahara may contribute to the mixing of particles of different origins.

#### 4 Summary and conclusions

Daily PM<sub>10</sub> samples collected at Lampedusa from 2004 to 2010 were analysed for selected elements and ions to determine the mineral contribution to PM<sub>10</sub> in the central Mediterranean Sea. From these data, the following conclusion can be drawn.

1. In spite of the distance from aerosol pollution sources, 10% of the total data number exceeded the daily threshold value ( $50\ \mu\text{g m}^{-3}$ , European Community, EC/30/1999) established by the European Commission for PM (35 days yr<sup>-1</sup>, corresponding to 9.6%).
2. The Saharan dust content was calculated as the sum of main oxides (Al, Si, Fe, Ti and non-sea-salt Ca, Na, Mg, K) for samples for which a PIXE analysis was performed. On average the crustal content accounts for  $5.42\ \mu\text{g m}^{-3}$ , and it may reach  $67.9\ \mu\text{g m}^{-3}$  during strong Saharan dust events.

3. Elevated Saharan dust events are identified from the nssCa concentration determined by ion chromatography. Non-sea-salt Ca presents a strong correlation with crustal aerosol determined as the sum of the metal oxides (slope  $10.0 \pm 2\%$   $R = 0.845$ ,  $n = 688$ ,  $p < 0.01$ ).
4. The crustal concentration determined from Al or Ca, using a fixed element-to-crustal concentration ratio, agrees well with the crustal amount calculated as the sum of the metal oxides. A large overestimate of the crustal content is derived by applying the EU guidelines for the subtraction of the dust events from the PM<sub>10</sub> limit exceedances to the Lampedusa data. This overestimate is produced by the high level of regional background aerosol concentration, which is higher than the 40th percentile value used in the background subtraction according to the EU guidelines.
5. The desert dust column burden displays an evident annual cycle, with a strong summer maximum. Conversely, the crustal aerosol amount contribution to PM<sub>10</sub> and the percentage of Saharan dust events do not show any evident seasonal pattern. We found that a high dust concentration is found at the ground in 71.3% of the events identified using the column optical properties, indicating that in many cases Saharan dust transport occurs above the marine boundary layer, and no significant mixing of the dust below and above the boundary layer takes place. This is especially true in summer when, due to the generally higher stability of the marine boundary layer, the greatest difference between boundary layer and free tropospheric dust evolution is observed.
6. Backward trajectories arriving at 50 m a.g.l. were analysed in connection with the dust chemical composition to identify possible differences in the properties of the dust source areas. Two main areas could be identified, corresponding to the Tunisia–Algeria region and to Libya. Transport from these regions takes place mainly in winter, when low altitude transport occurs. Data on the bulk composition of mineral aerosol from these two source areas are scarce; the present analysis shows a very large variability in the results, partly attributed to uncertainties in the trajectories and in the possible role of long-range transport over the Sahara. However, dust from the two sources present Ca/Al and Mg/Al ratios higher than for the mean upper crust composition. This is due to the presence in northern Africa region of carbonate and palygorskite (a Mg-bearing clay mineral) in areas with higher carbonate contents. Although the Ca/Al and especially (Ca+Mg)/Fe ratios present a large variability, they display a somewhat different behaviour in the two sources. The retrieved median value of Ca/Al and (Ca+Mg)/Fe are  $2.5 \pm 1.0$  and  $4.7 \pm 2.0$ , respectively, for dust aerosol

arising from Tunisia–Algeria; they are  $1.9 \pm 0.7$  and  $3.3 \pm 1.1$  (Ca/Al and (Ca+Mg)/Fe, respectively) for Libyan dust.

*Acknowledgements.* The study has been partially supported by the Italian Ministry of Education, Universities and Research through the SNUMMASS, NextData, and Ritmare Projects.

Edited by: N. Mihalopoulos

## References

- Abed, A. M., Al Kuisi, M., and Abul Khair, H.: Characterization of the Khamaseen (spring) dust in Jordan. *Atmos. Environ.*, 43, 2868–2876, 2009.
- Arola, A., Kazadzis, S., Lindfors A., Krotkov, N., Kujanpää, J., Tamminen, J., Bais, A., di Sarra, A., Villaplana, J. M., Brogniez, C., Siani, A. M., Janouch, M., Weihs, P., Koskela, T., Kouremeti, N., Meloni, D., Buchard, V., Auriol, F., Ialongo, I., Staneck, M., Simic, S., Webb, A., Smedley, A., and Kinne S.: A new approach to correct for absorbing aerosols in OMI UV, *Geophys. Res. Lett.*, 36, L22805, doi:10.1029/2009GL041137, 2009.
- Artuso, F., Chamard, P., Chiavarini, S., di Sarra, A., Meloni, D., Piacentino, S. and Sferlazzo, D. M.: Tropospheric halocarbons and nitrous oxide monitored at a remote site in the Mediterranean, *Atmos. Environ.*, 44, 4944–4953, 2010.
- Artuso, F., Chamard, P., Piacentino, S., Sferlazzo, D. M., De Silvestri, L., di Sarra, A., Meloni, D., and Monteleone, F.: Influence of transport and trends in atmospheric CO<sub>2</sub> at Lampedusa, *Atmos. Environ.*, 43, 3044–3051, 2009.
- Astitha, M., Kallos, G. and Katsafados, P.: Air pollution modeling in the Mediterranean Region: Analysis and forecasting of episodes, *Atmospheric Research*, 89, 358–364, 2008.
- Avila, A. and Rodà, F.: Assessing decadal changes in rainwater alkalinity at a rural Mediterranean site in the Montseny mountains (NE Spain), *Atmos. Environ.*, 36, 2881–2890, 2002.
- Baker, A. R. and Croot, P. L.: Atmospheric and marine controls on aerosol iron solubility in seawater, *Mar. Chem.*, 120, 4–13, doi:10.1016/j.marchem.2008.09.003, 2010.
- Becagli, S., Ghedini, C., Peeters, S., Rottiers, A., Traversi, R., Udisti, R., Chiari, M., Jalba, A., Despiou, S., Dayan, U., and Temara, A.: MBAS (Methylene Blue Active Substances) and LAS (Linear Alkylbenzene Sulphonates) in Mediterranean coastal aerosols: sources and transport processes, *Atmos. Environ.*, 45, 6788–6801, 2011.
- Becagli, S., Sferlazzo, D. M., Pace, G., di Sarra, A., Bommarito, C., Calzolari, G., Ghedini, C., Lucarelli, F., Meloni, D., Monteleone, F., Severi, M., Traversi, R., and Udisti, R.: Evidence for heavy fuel oil combustion aerosols from chemical analyses at the island of Lampedusa: a possible large role of ships emissions in the Mediterranean, *Atmos. Chem. Phys.*, 12, 3479–3492, doi:10.5194/acp-12-3479-2012, 2012.
- Bethoux, J. P. and Gentili, B.: The Mediterranean Sea, coastal and deep-sea signatures of climatic and environmental changes, *J. Marine Syst.*, 7, 383–394, 1996.
- Bethoux, J. P., Gentili, B., Morin, P., Nicolas, E., Pierre, C., and Ruiz-Pino, D.: The Mediterranean Sea: a miniature ocean for climatic and environmental studies and a key for the climatic functioning of the North Atlantic, *Prog. Oceanogr.*, 44, 131–146, 1999.
- Bethoux, J. P., Morin, P., and Ruiz-Pino, D. P.: Temporal trends in nutrient ratios: chemical evidence of Mediterranean ecosystem changes driven by human activity, *Deep Sea Res. II*, 49, 2007–2015, 2002.
- Bouchlaghem, K., Nsom, B., Latrache N., and Kacem, H. H.: Impact of Saharan dust on PM<sub>10</sub> concentration in the Mediterranean Tunisian coasts, *Atmos. Res.*, 92, 531–539, doi:10.1016/j.atmosres.2009.02.009, 2009.
- Bowen, H. J. M.: Environmental chemistry of the elements, Academic Press, 1979.
- Calzolari G., Chiari, M., García Orellana, I., Lucarelli, F., Migliori, A., Nava, S., and Taccetti, F.: The new external beam facility for environmental studies at the Tandatron accelerator of LABEC, *Nucl. Instr. Meth. B*, 249, 928–931, 2006.
- Canepari, S., Farao, C., Marconi, E., Giovannelli, C., and Perrino, C.: Qualitative and quantitative determination of water in airborne particulate matter, *Atmos. Chem. Phys.*, 13, 1193–1202, doi:10.5194/acp-13-1193-2013, 2013.
- Casasanta, G., di Sarra, A., Meloni, D., Monteleone, F., Pace, G., Piacentino, S., and Sferlazzo, D.: Large aerosol effects on ozone photolysis in the Mediterranean, *Atmos. Environ.*, 45, 3937–3943, 2011.
- Castillo, S., Moreno, T., Querol, X., Alastuey, A., Cuevas, E., Herrmann, L., Mounkaila, M., and Gibbons, W.: Trace element variation in size-fractionated African desert dusts, *J. Arid Environ.*, 72, 1034–1045, 2008.
- Claquin, T., Schulz, M., and Balkanski, Y. J.: Modeling the mineralogy of atmospheric dust sources, *J. Geophys. Res.*, 104, 22243–22256, 1999.
- Criado, C. and Dorta, P.: An unusual “blood rain” over the Canary Islands (Spain). The storm of January 1999, *J. Arid Environ.*, 55, 765–783, 2003.
- d’Almeida, G. A.: A Model for Saharan Dust Transport, *J. Climate Appl. Meteor.*, 25, 903–916, 1986.
- Dayan, U., Heffter, J. L., and Miller J. M.: Meteorological and climatological data from surface and upper measurements for the assessment of atmospheric transport and deposition of pollutants in the Mediterranean Basin: Part B: Seasonal distribution of the planetary boundary layer depths over the Mediterranean Basin, UNEP Mediterranean Action Plan Technical Reports Series no. 30, Athens, Greece, 1989.
- Dayan, U., Heffter, J., Miller, J., and Gutman, G.: Dust intrusion events into the Mediterranean Basin, *J. Appl. Meteorol.*, 30, 1185–1199, 1991.
- Dentener, F. J., Carmichael, G. R., Zhang, Y., Leleieveld, J., and Crutzen, P. J.: Role of mineral aerosols as a reactive surface in the global troposphere, *J. Geophys. Res.*, 101, 22869–22889, 1996.
- Desboeufs, K. V. and Cautenet, G.: Transport and mixing zone of desert dust and sulphate over Tropical Africa and the Atlantic Ocean region, *Atmos. Chem. Phys. Discuss.*, 5, 5615–5644, doi:10.5194/acpd-5-5615-2005, 2005.
- Di Biagio, C., di Sarra, A., and Meloni, D.: Large atmospheric shortwave radiative forcing by Mediterranean aerosol derived from simultaneous ground-based and spaceborne observations, and dependence on the aerosol type and single scattering albedo,

- J. Geophys. Res., 115, D10209, doi:10.1029/2009JD012697, 2010.
- Di Iorio, T., di Sarra, A., Sferlazzo, D. M., Cacciani, M., Meloni, D., Monteleone, F., Fuà, D., and Fiocco, G.: Seasonal evolution of the tropospheric aerosol vertical profile in the central Mediterranean and role of desert dust, J. Geophys. Res., 114, D02201, doi:10.1029/2008JD010593, 2009.
- di Sarra, A., Cacciani, M., Chamard, P., Cornwall, C., DeLuisi, J. J., Di Iorio, T., Disterhoft, P., Fiocco, G., Fuà, D., and Monteleone, F.: Effects of desert dust and ozone on the ultraviolet irradiance at the Mediterranean island of Lampedusa during PAUR II, J. Geophys. Res., 107, 8135, doi:10.1029/2000JD000139, 2002.
- di Sarra, A., Pace, G., Meloni, D., De Silvestri, L., Piacentino, S., and Monteleone, F.: Surface shortwave radiative forcing of different aerosol types in the central Mediterranean, Geophys. Res. Lett., 35, L02714, doi:10.1029/2007GL032395, 2008.
- di Sarra, A., Di Biagio, C., Meloni, D., Monteleone, F., Pace, G., Pugnaghi, S., and Sferlazzo, D.: Shortwave and longwave radiative effects of the intense Saharan dust event of 25–26 March 2010 at Lampedusa (Mediterranean sea), J. Geophys. Res., 116, D23209, doi:10.1029/2011JD016238, 2011.
- Draxler, R. R. and Rolph, G. D.: HYSPLIT (HYbrid Single-Particle Lagrangian Integrated Trajectory) Model access via NOAA ARL READY Website <http://ready.arl.noaa.gov/HYSPLIT.php>, NOAA Air Resources Laboratory, Silver Spring, MD, 2012.
- Duce, R. A., Liss, P. S., Merrill, J. T., Buat-Menard, P., Hicks, B. B., Miller, J. M., Prospero, J. M., Arimoto, R., Church, T. M., Ellis, W., Galloway, J. N., Hanson, K., Jickells, T. D., Knapp, A. H., Rienhart, K. H., Schneider, B., Soudine, A., Tokos, J. J., Tsunogai, S., Wollast, R., and Zhou, M.: The atmospheric input of trace species to the world ocean, Global Biogeochem. Cy., 5, 193–259, 1991.
- Eldred, R. A., Cahill, T. A., and Feeney, P. J.: Particulate monitoring at US National Parks using PIXE, Nucl. Instr. Meth. B, 22, 289–295, 1987.
- Engelstaedter, S. and Washington, R.: Atmospheric controls on the annual cycle of North African dust, J. Geophys. Res., 112, D03103, doi:10.1029/2006JD007195, 2007.
- Engelstaedter, S., Tegen, I., and Washington, R.: North African dust emissions and transport, Earth Sci. Rev., 79, 73–100, 2006.
- Engelstaedter, S., Tegen, I., and Washington, R.: North African dust emissions and transport, Earth-Science Rev., 79, 73–100, 2006.
- Erel, Y., Dayan, U., Rabi, R., Rudich, Y., and Stein, M.: Trans boundary transport of pollutants by atmospheric mineral dust, Environ. Sci. Technol., 40, 2996–3005, 2006.
- Escudero, M., Castillo, S., Querol, X., Avila, A., Alarcoñ, M., Viana, M. M., Alastuey, A., Cuevas, E., and Rodríguez, S.: Wet and dry African dust episodes over Eastern Spain, J. of Geophys. Res., 110, D18S08, doi:10.1029/2004JD004731, 2005.
- Escudero, M., Querol, X., Avila, A., and Cuevas, E.: Origin of the exceedances of the European daily PM limit value in the regional background areas of Spain, Atmos. Environ., 41, 730–744, 2007.
- Escudero, M., Stein, A. F., Draxler, R. R., Querol, X., Alastuey, A., Castillo, S., and Avila, A.: Source apportionment for African dust outbreaks over the Western Mediterranean using the HYSPLIT model, Atmos. Res., 99, 518–527, 2011.
- European Community, the Air Quality Directive (Directive 1999/30/EC). Official Journal of the European Communities 29. 6. 1999 L 163/41 COUNCIL DIRECTIVE 1999/30/EC of 22 April 1999, <http://eur-lex.europa.eu/LexUriServ/LexUriServ.do?uri=OJ:L:1999:163:0041:0060:EN:PDF>, 1999.
- Fairlie, T. D., Jacob, D. J., Dibb, J. E., Alexander, B., Avery, M. A., van Donkelaar, A., and Zhang, L.: Impact of mineral dust on nitrate, sulphate, and ozone in transpacific Asian pollution plumes, Atmos. Chem. Phys., 10, 3999–4012, doi:10.5194/acp-10-3999-2010, 2010.
- Favez, O., Cachier, H., Sciare, J., Alfaro S. C., El-Araby, T. M., Harhash, M. A., and Abdelwahab M. M.: Seasonality of major aerosol species and their transformations in Cairo megacity, Atmos. Environ., 42, 1503–1516, 2008.
- Gallissai, R., Peters, F., Basart, S., and Baldasano, J. M.: Mediterranean basin-wide correlations between Saharan dust deposition and ocean chlorophyll concentration, Biogeosciences Discuss., 9, 8611–8639, doi:10.5194/bgd-9-8611-2012, 2012.
- Ganor, E., and Foner, H. A.: The mineralogical and chemical properties and the behaviour of aeolian Saharan dust over Israel, in: Guerzoni, S., Chester, R. (Eds.), The Impact of Desert Dust Across the Mediterranean. Kluwer Academic Publishers, Dordrecht, the Netherlands, 1996.
- Gerasopoulos, E., Kouvarakis, G., Babasakalis, P., Vrekoussis, M., Putaud, J.-P., and Mihalopoulos, N.: Origin and variability of particulate matter (PM<sub>10</sub>) mass concentrations over the Eastern Mediterranean, Atmos. Environ., 40, 4679–4690, 2006.
- Gobbi, G. P., Barnaba, F., Giorgi, R., and Santacasa, A.: Altitude resolved properties of a Saharan dust event over the Mediterranean, Atmos. Environ., 34, 5119–5127, doi:10.1016/S1352-2310(00)00194-1, 2000.
- Gómez-Amo, J. L., Estellés, V., di Sarra, A., Pedrós, R., Utrillas, M. P., Martínez-Lozano, J. A., González-Frias, C., Kyrö, E., and Vilaplana, J. M.: Operational considerations to improve total ozone measurements with a Microtops II ozone monitor, Atmos. Meas. Tech., 5, 759–769, doi:10.5194/amt-5-759-2012, 2012.
- Guerzoni, S., Chester, R., Dulac, F., Herut, B., Loye-Pilot, M.-D., Measures, C., Migon, C., Molinaroli, E., Moulin, C., Rossini, P., Saydam, C., Soudine, A., and Ziveri, P.: The role of atmospheric deposition in the biogeochemistry of the Mediterranean Sea, Prog. Oceanogr., 44, 147–190, 1999.
- Guinot, B., Cachier, H., and Oikonomou, K.: Geochemical perspectives from a new aerosol chemical mass closure, Atmos. Chem. Phys., 7, 1657–1670, doi:10.5194/acp-7-1657-2007, 2007.
- Harrison, L., Michalsky, J., and Berndt, J.: Automated multifilter rotating shadowband radiometer: an instrument for optical depth and radiation measurements, Appl. Opt., 33, 5118–5125, 1994.
- Henderson, P. and Henderson, G. M.: The Cambridge Handbook of Earth Science Data, Cambridge, University Press, Cambridge, 42–44, 2009.
- IPCC – Climate Change 2007: the Physical Science Basis. Contribution of Working Group I to the Fourth Assessment Report of the IPCC.
- Israelevich, P. L., Levin, Z., Joseph, J. H., and Ganor, E.: Desert aerosol transport in the Mediterranean region as inferred from the TOMS aerosol index, J. Geophys. Res., 107, 4572, doi:10.1029/2001JD002011, 2002.
- Kallos, G., Astitha, M., Katsafados, P., and Spyrou, C.: Long-Range transport of Anthropogenically and Naturally Produced particulate matter in the Mediterranean and north Atlantic: current State of Knowledge, J. Appl. Meteorol. Clim., 46, 1230–1251, doi:10.1175/JAM2530.1, 2007.

- Khiri, F., Ezaidi, A., and Kabbachi, K.: Dust deposits in Sous–Massa basin, South-West of Morocco: granulometrical, mineralogical and geochemical characterization, *J. Afr. Earth Sci.*, 39, 459–464, 2004.
- Koçak, M., Mihalopoulos, N., and Kubilay, N.: Contributions of natural sources to high PM<sub>10</sub> and PM<sub>2.5</sub> events in the eastern Mediterranean, *Atmos. Environ.*, 41, 3806–3818, 2007.
- Koulouri, E., Saarikoski S., Theodosi C., Markaki Z., Gerasopoulos, E., G. Kouvarakis, Mäkelä, T., Hillamo, R., and Mihalopoulos, N.: Chemical composition and sources of fine and coarse aerosol particles in the Eastern Mediterranean, *Atmos. Environ.*, 42, 6542–6550, 2008.
- Kouvarakis, G., Tsigaridis, K., Kanakidou, M., and Mihalopoulos, N.: Temporal variations of surface regional background ozone over Crete Island in southeast Mediterranean, *J. Geophys. Res.*, 105, 4399–4407, 2000.
- Lelieveld, J. and Dentener, F. J.: What controls tropospheric ozone?, *J. Geophys. Res.*, 105, 3531–3551, 2000.
- Levin, Z., Ganor, E., and Gladstein, V.: The effects of desert particles coated with sulfate on rain formation in the Eastern Mediterranean, *J. Appl. Meteorol.*, 35, 1511–1523, 1996.
- Linke, C., Möhler, O., Veres, A., Mohácsi, Á., Bozóki, Z., Szabó, G., and Schnaiter, M.: Optical properties and mineralogical composition of different Saharan mineral dust samples: a laboratory study, *Atmos. Chem. Phys.*, 6, 3315–3323, doi:10.5194/acp-6-3315-2006, 2006.
- Lucarelli, F., Nava, S., Calzolari, G., Chiari, M., Udusti, R., and Marino, F.: Is PIXE still a useful technique for the analysis of atmospheric aerosols? The LABEC experience, *X-Ray Spectrometry*, 40, 162–167, doi:10.1002/xrs.1312, 2011.
- Malm, W. C., Sisler, J. F., Huffman, D., Eldred, R. A., and Cahill, T. A.: Spatial and seasonal trends in particle concentration and optical extinction in the United States, *J. Geophys. Res.*, 99, 1347–1370, 1994.
- Marcazzan, G. M., Vaccaro, S., Valli, G., and Vecchi, R.: Characterisation of PM<sub>10</sub> and PM<sub>2.5</sub> particulate matter in the ambient air of Milan (Italy), *Atmos. Environ.*, 35, 4639–4650, 2001.
- Marticorena, B., Bergametti, G., Aumont, B., Callot, Y., N'Doumé C., and Legrand M.: Modelling the atmospheric dust cycle : 2-Simulations of Saharan dust sources, *J. Geophys. Res.*, 102, 4387–4404, 1997.
- Mateos, D., Bilbao J., Kudish, A. I., Parisi, A. V., Carbajal, G., di Sarra, A., Román, R., and de Miguel, A.: Validation of satellite erythral radiation retrievals using ground-based measurements in five countries, *Remote Sens. Environ.*, 128, 1–10, 2013.
- Meloni, D., di Sarra, A., Herman, J. R., Monteleone, F., and Piacentino, S.: Comparison of ground-based and TOMS erythral UV doses at the island of Lampedusa in the period 1998–2003: Role of tropospheric aerosols, *J. Geophys. Res.*, 110, D01202, doi:10.1029/2004JD005283, 2005.
- Meloni, D., di Sarra, A., Biavati, G., De Luisi, J. J., Monteleone, F., Pace, G., Piacentino, S., Sferlazzo, D.: Seasonal behaviour of Saharan dust events at the Mediterranean island of Lampedusa in the period 1999–2005, *Atmos. Environ.*, 41, 3041–3056, 2007.
- Meloni, D., di Sarra, A., Fiocco, G., and Junkermann, W.: Tropospheric aerosols in the Mediterranean: III. Measurements and modeling of actinic radiation profiles, *J. Geophys. Res.*, 108, 4323, doi:10.1029/2002JD003293, 2003.
- Meloni, D., di Sarra, A., Monteleone, F., Pace, G., Piacentino, S., and Sferlazzo, D. M.: Seasonal transport patterns of intense Saharan dust events at the Mediterranean island of Lampedusa, *Atmos. Res.*, 88, 134–148, doi:10.1016/j.atmosres.2007.10.007, 2008.
- Meloni, D., di Sarra, A., Pace, G., and Monteleone, F.: Optical properties of aerosols over the central Mediterranean. 2. Determination of single scattering albedo at two wavelengths for different aerosol types, *Atmos. Chem. Phys.*, 6, 715–727, doi:10.5194/acp-6-715-2006, 2006.
- Miranda, J., Cahill, T. A., and Morales, J. R.: Determination of elemental concentrations in atmospheric aerosols in Mexico City using proton induced X-Ray emission, proton Elastic scattering and Laser absorption, *Atmos. Environ.*, 28, 2299–2306, 1994.
- Moreno, T., Querol, X., Castillo, S., Alastuey, A., Cuevas, E., Herrmann, L., Mounkaila, M., Elvira, J., and Gibbons, W.: Geochemical variations in aeolian mineral particles from the Sahara–Sahel dust corridor, *Chemosphere*, 65, 261–270, 2006.
- Nava, S., Becagli, S., Calzolari, G., Chiari, M., Lucarelli, F., Prati, P., Traversi, R., Udusti, R., Valli G., and Vecchi R.: Saharan dust impact in central Italy: An overview on three years elemental data Records, *Atmos. Environ.*, 60, 444–452, 2012.
- Pace, G., Meloni, D., and di Sarra, A.: Forest fire aerosol over the Mediterranean basin during summer 2003, *J. Geophys. Res.*, 110, D21202, doi:10.1029/2005JD005986, 2005.
- Pace, G., di Sarra, A., Meloni, D., Piacentino, S., and Chamard, P.: Aerosol optical properties at Lampedusa (Central Mediterranean). 1. Influence of transport and identification of different aerosol types, *Atmos. Chem. Phys.*, 6, 697–713, doi:10.5194/acp-6-697-2006, 2006.
- Pace, G., Cremona, G., di Sarra, A., Meloni, D., Monteleone, F., Sferlazzo, D., and Zanini, G.: Continuous vertical profiles of temperature and humidity at Lampedusa island, Proceedings of the 9th International Symposium on Tropospheric Profiling, L'Aquila, Italy, September 2012.
- Papayannis, A., Amiridis, V., Mona, L., Tsaknakis, G., Balis, D., Bösenberg, J., Chaikovski, A., De Tomasi, F., Grigorov, I., Mattis, I., Mitev, V., Müller, D., Nickovic, S., Pérez, C., Pietruczuk, A., Pisani, G., Ravetta, F., Rizi, V., Sicard, M., Trickl, T., Wiegner, M., Gerding, M., Mamouri, R. E., D'Amico, G., and Pappalardo, G.: Systematic lidar observations of Saharan dust over Europe in the frame of EARLINET (2000–2002), *J. Geophys. Res.*, 113, D10204, doi:10.1029/2007JD009028, 2008.
- Pederzoli, A., Mircea, M., Finardi, S., di Sarra, A., and Zanini, G.: Quantification of Saharan dust contribution to PM<sub>10</sub> concentrations over Italy in 2003–2005, *Atmos. Environ.*, 44, 4181–4190, 2010.
- Perrino, C., Canepari, S., Cardarelli, E., Catrambone, M., and Sagolini, T.: Inorganic constituents of urban air pollution in the Lazio region (Central Italy), *Environ Monit. Assess.*, 136, 69–86, 2008.
- Pey, J., Querol, X., Alastuey, A., Forastiere, F., and Stafoggia, M.: African dust outbreaks over the Mediterranean Basin during 2001–2011: PM<sub>10</sub> concentrations, phenomenology and trends, and its relation with synoptic and mesoscale meteorology, *Atmos. Chem. Phys.*, 13, 1395–1410, doi:10.5194/acp-13-1395-2013, 2013.
- Putaud, J.-P., Van Dingenen, R., Dell'Acqua, A., Raes, F., Matta, E., Decesari, S., Facchini, M. C., and Fuzzi, S.: Size-segregated

- aerosol mass closure and chemical composition in Monte Cimone (I) during MINATROC, *Atmos. Chem. Phys.*, 4, 889–902, doi:10.5194/acp-4-889-2004, 2004.
- Querol, X., Peya, J., Pandolfi, M., Alastuey, A., Cusack, M., Perez, N., Moreno, T., Viana, M., Mihalopoulos, N., Kallos, G., and Kleanthous, S.: African dust contributions to mean ambient  $PM_{10}$  mass-levels across the Mediterranean Basin, *Atmos. Environ.*, 43, 4266–4427, 2009.
- Rodríguez, S., Alastuey, A., Alonso-Pérez, S., Querol, X., Cuevas, E., Abreu-Afonso, J., Viana, M., Perez, N., Pandolfi, M., and de la Rosa, J.: Transport of desert dust mixed with North African industrial pollutants in the subtropical Saharan Air Layer, *Atmos. Chem. Phys.*, 11, 6663–6685, doi:10.5194/acp-11-6663-2011, 2011.
- Rodríguez, S., Alastuey, A., and Querol, X.: A review of methods for long term in situ characterization of aerosol dust, *Aeolian Res.*, 6, 55–74, 2012.
- Rodríguez, S., Querol, X., Alastuey, A., Kallos, G., and Kakaliagou, O.: Saharan dust contributions to  $PM_{10}$  and TSP levels in Southern and Eastern Spain, *Atmos. Environ.*, 35, 2433–2447, 2001.
- Scheuven, D., Schütz, L., Kandler, K., Ebert, M., and Weinbruch, S.: Bulk composition of northern African dust and its source sediments – A compilation, *Earth-Science Rev.*, 116, 170–194, 2013.
- Sciare, J., Oikonomou, K., Cachier, H., Mihalopoulos, N., Andreae, M. O., Maenhaut, W., and Sarda-Estève, R.: Aerosol mass closure and reconstruction of the light scattering coefficient over the Eastern Mediterranean Sea during the MINOS campaign, *Atmos. Chem. Phys.*, 5, 2253–2265, doi:10.5194/acp-5-2253-2005, 2005.
- Sharif, S.: Chemical and mineral composition of dust and its effect on the dielectric constant, *IEEE Trans. Geosci. Remote Sens.*, 33, 353–358, 1995.
- Tomadin, L., Cesari, G., Fuzzi, S., Landuzzi, V., Lenaz, R., Lobiatti, A., Mandrioli, P., Mariotti, M., Mazzucotelli, A., and Vannucci, R.: Eolian dust collected in springtime (1979 and 1984 years) at the seawater–air interface of the Northern Red Sea edited by: Leinen, M., Sarnthein, M., *Palaeoclimatology and Palaeometeorology: Modern and Past Patterns of Global Atmospheric Transport*. NATO ASI Series C, 282, Kluwer Academic Publishers, Dordrecht, the Netherlands, 1989.
- Tsyro, S. G.: To what extent can aerosol water explain the discrepancy between model calculated and gravimetric  $PM_{10}$  and  $PM_{2.5}$ , *Atmos. Chem. Phys.*, 5, 515–532, doi:10.5194/acp-5-515-2005, 2005.
- Wagener, T., Guieu, C., and Leblond N.: Effects of dust deposition on iron cycle in the surface Mediterranean Sea: results from a mesocosm seeding experiment, *Biogeosciences*, 7, 3769–3781, doi:10.5194/bg-7-3769-2010, 2010.
- Zender, C. S., Miller, R. L., and Tegen, I.: Quantifying mineral dust mass budgets: Terminology, constraints, and current estimates, *Eos Trans. Amer. Geophys. Union*, 85, 48, 509–512, 2004.